Dynamic Analysis of Planetary-Type Magnetic Gear Based on Reluctance Network Analysis

Michinari Fukuoka, Kenji Nakamura, and Osamu Ichinokura

Tohoku University, Graduate School of Engineering, 6-6-05 Aoba Aramaki Aoba-ku, Sendai 980-8579, Japan

Magnetic gears are able to transmit torque without mechanical contact. Therefore, these have attractive features, such as low acoustic noise and maintenance-free operation in comparison with conventional mechanical gears. Planetary-type magnetic gears, especially, have higher transmission torque than the other types, and are expected to be put into practical use. This paper presents a method for calculating dynamic characteristics of the magnetic gear based on reluctance network analysis (RNA). The RNA has several features, including a simple analytical model, high calculation accuracy, and ease of coupled analysis with rotational motion of rotors.

***Index Terms*—Dynamic analysis, magnetic gear, reluctance network analysis (RNA).**

I. INTRODUCTION

MECHANICAL gears are widely used in various applications to obtain required torque and speed. However, these have some problems, including vibration and acoustic noise due to mechanical contact. In addition, the mechanical gears require the cooling system in high-power applications.

On the other hand, magnetic gears can transmit torque without mechanical contact. Therefore, vibration and acoustic noise are very low, and gear lubricant is not required. Various types of magnetic gears have been introduced in previous papers [1]–[3]. Among them, a planetary-type magnetic gear [4] has attracted interest recently.

The planetary-type magnetic gear consists of inner and outer rotors with mounted permanent magnets (PMs), and ferromagnetic stationary parts which are called pole pieces. It transmits torque by modulating the PM fluxes with the pole pieces. Transmission torque density of the planetary-type magnetic gear is higher than the other types because all of the PMs of the inner and outer rotors contribute to generate and transmit torque [5], [6].

In the future, the planetary-type magnetic gear is expected to be put into practical use. Therefore, the establishment of a dynamic analysis method of the magnetic gear is necessary. These days, a number of general-purpose programs of finite-element analysis (FEA) have been placed on the market. However, FEA-based dynamic analysis, including motion equation, is difficult because its analytical model is complicated and calculation time tends to be long.

Reluctance network analysis (RNA) is one of the practical solutions because the analytical model is simple, calculation accuracy is relatively high, and it is easy to combine with motion dynamics [7].

In this paper, we propose the RNA model of the planetary-type magnetic gears first, and then calculated torque is compared to that obtained from FEA. Finally, the RNA-based dynamic analysis method of the magnetic gear is presented.

Manuscript received February 21, 2011; revised May 06, 2011; accepted May 10, 2011. Date of current version September 23, 2011. Corresponding author: M. Fukuoka (e-mail: power20@ec.ecei.tohoku.ac.jp).

Color versions of one or more of the figures in this paper are available online at http://ieeexplore.ieee.org.

Digital Object Identifier 10.1109/TMAG.2011.2157100

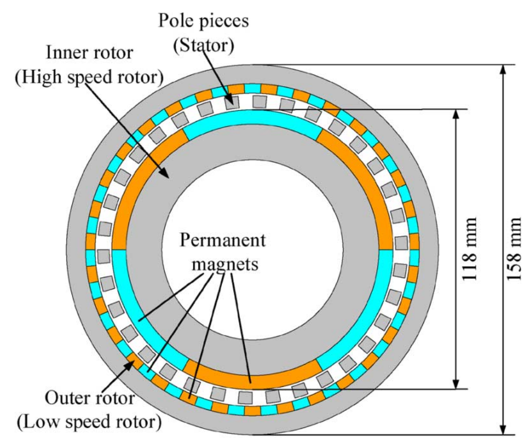

Stack length :	10 mm
Airgap length :	1 mm
Inner magnet pole-pair :	3
Outer magnet pole-pair :	31
The number of Pole-pieces :	34
Gear ratio :	1 : 10.333
Permanent magnet (Nd-Fe-B)	
Residual magnetic flux density :	1.25 T
Coercive force :	975 kA/m

Fig. 1. Structure and specifications of a planetary-type magnetic gear.

II. RNA MODEL OF THE MAGNETIC GEAR AND ANALYSIS

A. *RNA Model of the Planetary-Type Magnetic Gear*

Fig. 1 shows the structure and specifications of the planetary-type magnetic gear used in the consideration. The inner and outer rotors have permanent magnets on their surfaces. The numbers of pole pairs of the inner and outer rotors are 3 and 31, respectively. Hence, the gear ratio is 1:10.333, which is given by the ratio of the inner and outer pole pairs [5]. The pole pieces are placed between the inner and outer rotors. The number of pole pieces is 34, which is given by the sum of the inner and outer pole pairs. The material of the permanent magnet is Nd-Fe-B of which residual flux density B_r is 1.25 T and coercive force H_c is 975 kA/m. The core material of the pole pieces and the rotor back yoke is nonoriented silicon steel.

In order to derive the RNA model, first of all, the magnetic gear is divided into multiple elements as shown in Fig. 2. The number of divisions in a circumferential direction is determined based on the number of the pole pieces so that the pole pieces are divided uniformly into an integral number. On the other hand,

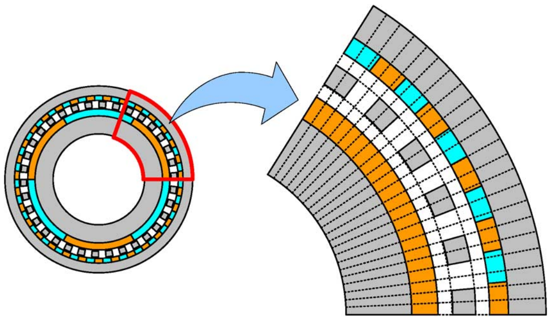

Fig. 2. Divisions of the magnetic gear based on RNA.

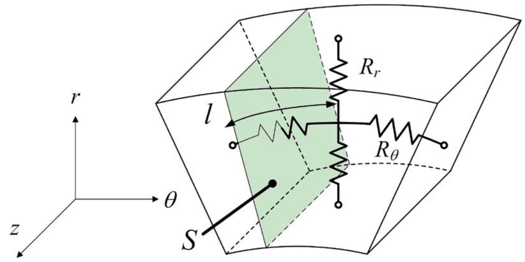

Fig. 3. Unit magnetic circuit.

it is not necessary to divide the rotor magnets uniformly into an integral number because the magnetomotive forces (MMFs) of permanent magnets are given by a continuous function of a rotor position angle θ in the RNA model.

Each divided element is expressed in a 2-D unit magnetic circuit as shown in Fig. 3. The reluctances R_r and R_θ in the circuit are given by only the dimensions of the divided element and the $B-H$ curve of core material as shown in the following nonlinear equation [7]:

$$R(\phi) = \frac{\alpha_1 l}{S} + \frac{\alpha_{13} l}{S^{13}} \phi^{12} \tag{1}$$

where the cross section is S, and the magnetic path length is l, respectively. The coefficients α_1 and α_{13} are 58 and 5, which can be obtained from the $B-H$ curve of core material.

Fig. 4 shows the expanded view of the RNA model obtained in the way described before. The number of divisions in a circumferential direction is 476, that is, each pole piece is divided into seven parts.

The MMF of permanent magnet f_c is defined by

$$f_c = H_c l_m \tag{2}$$

where the length of the magnet is l_m. Thus, the MMFs F_l and F_h are given by the following function so that the rotary motion can be considered in the RNA model:

$$\begin{aligned} F_k &= H_c(\theta) l_{mk} \\ &= H_c l_{mk} \times \frac{2}{\pi} \tan^{-1}(b_k \sin p_k \theta) \quad (k = l, h), \end{aligned} \tag{3}$$

where the coefficients b_h and b_l are 2 and 1, respectively, and the number of pole pairs is p_k.

B. Steady-State Analysis

Fig. 5 shows the flow diagram of steady-state analysis using the RNA model. When the angular velocities of the inner and outer rotors ω_h, ω_l are given first, both rotor positions θ_h, θ_l are obtained from

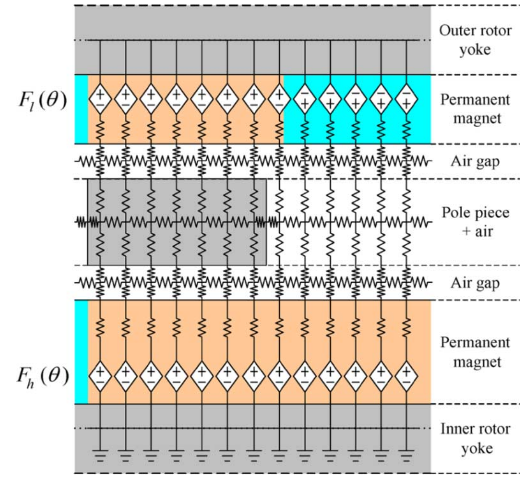

Fig. 4. Expanded view of the RNA model of the magnetic gear.

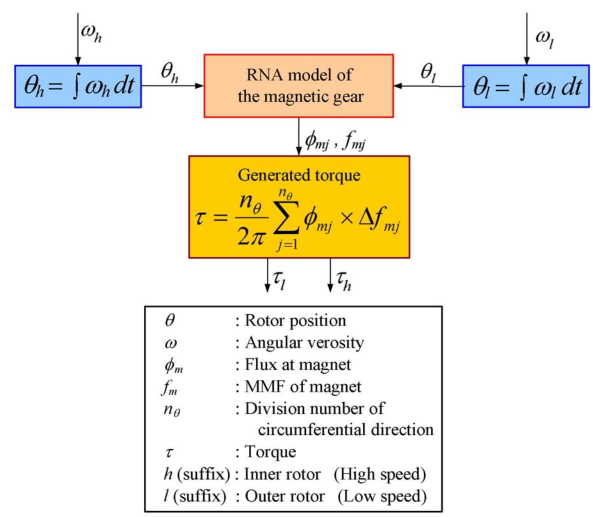

Fig. 5. Flow diagram of steady-state simulation based on RNA.

$$\theta_k = \int \omega_k dt \quad (k = h, l). \tag{4}$$

Next, flux distribution in the RNA model of the magnetic gear is calculated, and then the generated torque of both rotors is calculated by the following function based on magnetic energy [8]:

$$\tau = \frac{n_\theta}{2\pi} \sum_{j=1}^{n_\theta} \phi_{mj} \times \Delta f_{mj}, \tag{5}$$

where the number of rotor divisions in the circumferential direction is n_θ. The fluxes and MMFs in the permanent magnets are ϕ_{mj} and f_{mj}, respectively. All of the calculations just shown can be performed simultaneously on SPICE which is a general-purpose circuit simulator.

Fig. 6 shows the transmission torque characteristic calculated by RNA and FEA. The internal phase angle is presented as the difference between the d-axes of the inner and outer rotors. It is understood that the maximum transmission torque is obtained when an internal phase angle is 90° in the same manner as

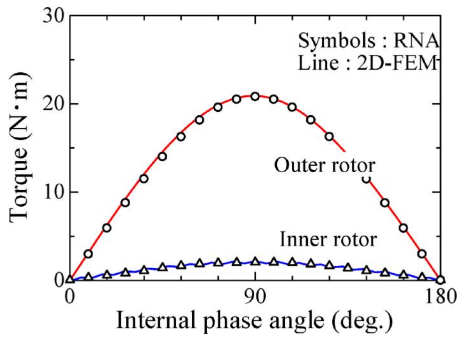

Fig. 6. Transmission torque characteristic calculated by RNA and FEM.

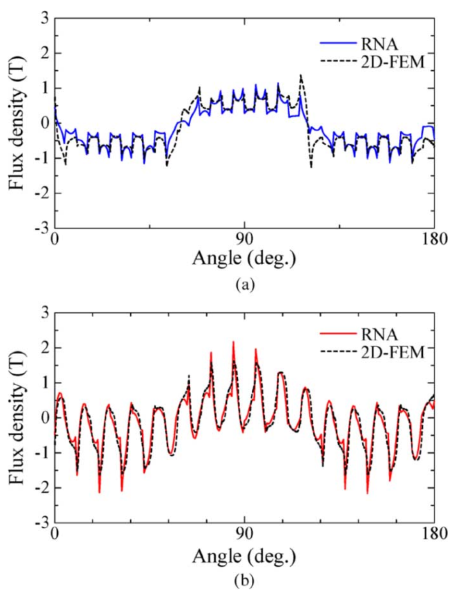

Fig. 7. Variation of the radial component of resulting flux density in two air gaps. (a) The gap between the inner rotor and pole pieces. (b) The gap between outer rotor and pole pieces.

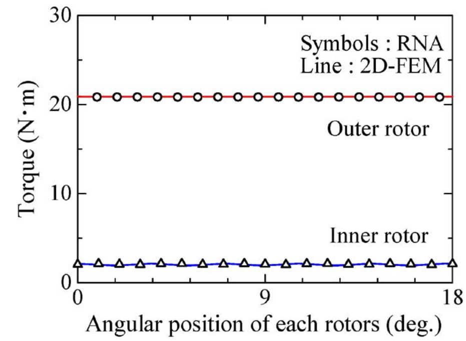

Fig. 8. Calculated variation of the maximum torque obtained from RNA and FEM.

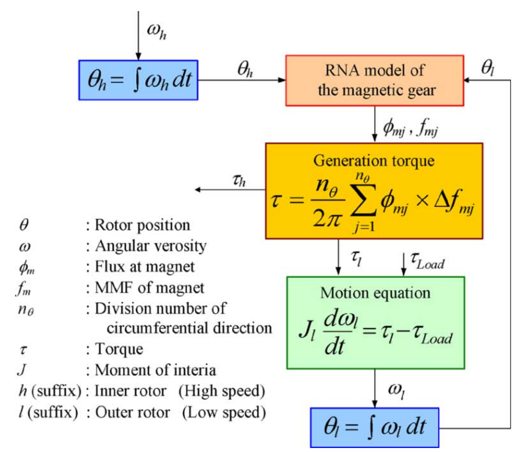

Fig. 9. Flow diagram of the dynamic simulation based on RNA.

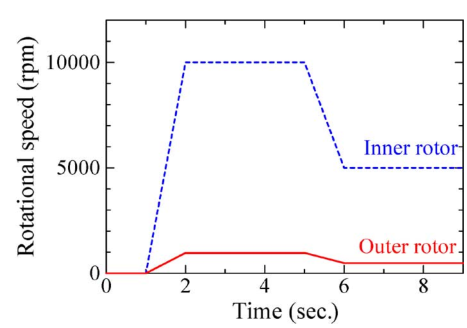

Fig. 10. Rotational speed behavior obtained from the RNA-based dynamic simulation.

synchronous machines. The figure reveals that both calculated values are in good agreement. The computation times of RNA and FEA are a few seconds and about 30 min, respectively.

Fig. 7 indicates the calculated variation of the radial component of resulting flux density in the inner and outer air gaps at the maximum output point where the internal phase angle is 90°. It is understood that the complicated distribution in the gap can be well predicted by RNA.

Fig. 8 shows the calculated variation of the maximum torque which is exerted on the inner and outer rotors as they rotate. It is clear that the torque ripple is very small.

C. Dynamic Analysis

Fig. 9 illustrates the flow diagram of dynamic analysis using the RNA model. First of all, when the angular velocity of the inner rotor ω_h is given, the inner rotor position θ_h is calculated by (4). Next, flux distribution in the RNA model of the magnetic gear is calculated, and then the generated torques of both rotors τ_h, τ_l are calculated by (5). After that, the angular velocity of the outer rotor ω_l is obtained from the motion equation

$$J_l \frac{d\omega_l}{dt} = \tau_l - \tau_{\mathrm{Load}}, \tag{6}$$

where the moment of inertia of the outer rotor J_l is $2.16 \times 10^{-3}\ \mathrm{kg} \cdot \mathrm{m}^2$, and the load torque is τ_{Load}. Finally, the outer rotor position θ_l is calculated by (4) using ω_l.

Fig. 10 shows the rotational speed behavior at no load obtained from the RNA-based dynamic simulation. The figure reveals that the outer rotor is rotated following the rotational speed of the inner rotor while keeping a gear ratio of 1: 10.333.

Fig. 11 shows the torque behavior at a constant speed of 1000 r/min. It is indicated that the gear can transmit the required torque of a ratio of 1:10.333 below the maximum torque;

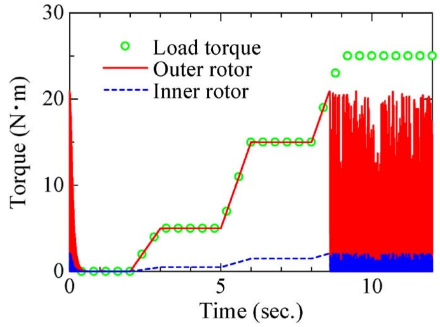

Fig. 11. Torque behavior obtained from the RNA-based dynamic simulation.

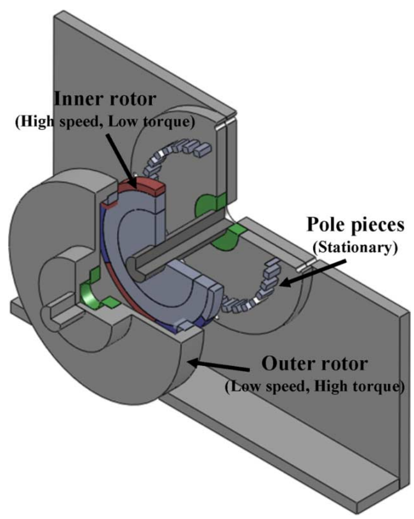

Fig. 12. Structure of the trial planetary magnetic gear.

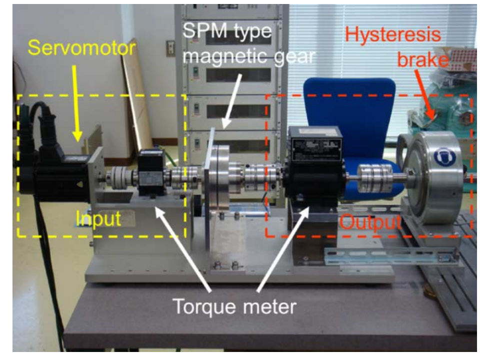

Fig. 13. General view of an experimental system with the trial magnetic gear.

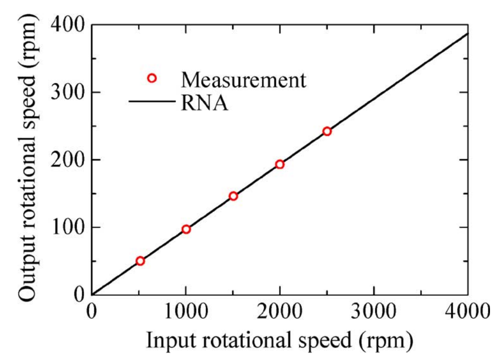

Fig. 14. Speed characteristics obtained from RNA-based simulation and measurement.

however, the gear loses synchronism when the load exceeds the pull-out torque.

III. Experimental Result

On the basis of the aforementioned results, a trial planetary-type magnetic gear was made. Fig. 12 illustrates the structure of the magnetic gear, which has the same specifications shown in Fig. 1.

Fig. 13 shows the general view of the experimental setup. The trial magnetic gear operates as a reduction gear on this system. The rotational speed of the inner rotor is given by the servomotor. The load torque is controlled by the hysteresis brake.

Fig. 14 shows the input rotational speed versus output rotational speed. It is understood from the figure that the ratio of the inner and outer rotor speed is 1: 10.333, and that the measured and calculated values are in good agreement.

IV. Conclusion

This paper presented a method for calculating the dynamic characteristics of the planetary-type magnetic gear based on RNA. The calculated values obtained from the proposed method agree well with that given by FEA. This work was supported by JSPS Grant-in-Aid for Challenging Exploratory Research (21656070).

References

[1] D. E. Hesmondhalgh and D. Tipping, “A multielement magnetic gear,” *Proc. Inst. Elect. Eng., Elect. Power Appl.*, vol. 127, p. 129, 1980.
[2] K. Tsurumoto and S. Kikushi, “A new magnetic gear using permanent magnet,” *IEEE Trans. Magn.*, vol. MAG-23, no. 5, p. 3622, Sep. 1987.
[3] K. Ikuta, S. Makita, and S. Arimoto, “Non-contact magnetic gear for micro transmission mechanism,” in *Proc. IEEE Conf. Micro Electromechan. Syst.*, 1991, p. 125.
[4] T. B. Martin Jr., “Magnetic transmission,” U.S. Patent 3 378 710, Apr. 16, 1968.
[5] K. Atallah and D. Howe, “A novel high-performance magnetic gear,” *IEEE Trans. Magn.*, vol. 37, no. 4, pt. 1, pp. 2844–2846, Jul. 2001.
[6] K. Atallah, S. D. Calverley, and D. Howe, “Design, analysis and realisation of a high-performance magnetic gear,” *Proc, Inst. Elect. Eng., Elect. Power Appl*, vol. 151, p. 135, 2004.
[7] K. Nakamura and O. Ichinokura, “Dynamic simulation of PM motor drive system based on reluctance network analysis,” in *Proc. EPE-PEMC*, 2008, p. 441.
[8] K. Nakamura, M. Ishihara, and O. Ichinokura, “Reluctance network analysis model of a permanent magnet generator considering an overhang structure and iron loss,” in *Proc. 17th Int. Conf. Elect. Mach.*, Chania, Greece, 2006, vol. PSA1-16.